



**POLITECNICO**  
MILANO 1863

SCUOLA DI INGEGNERIA INDUSTRIALE  
E DELL'INFORMAZIONE

EXECUTIVE SUMMARY OF THE THESIS

## Thermal stability of size- and termination-selected polyynes embedded in polymeric nanocomposite films monitored via *in situ* SERS mapping

LAUREA MAGISTRALE IN MATERIALS ENGINEERING AND NANOTECHNOLOGY - INGEGNERIA DEI MATERIALI E DELLE NANOTECNOLOGIE

**Author:** ALICE CARTOCETI

**Advisor:** PROF. CARLO S. CASARI

**Co-advisor:** PIETRO MARABOTTI

**Academic year:** 2021-2022

### 1. Introduction

Polyynes are one of the two possible isomeric forms of carbyne, the 1D allotrope of carbon. These systems are constituted by one-dimensional finite chains made of sp-hybridised carbon atoms, bound through alternated single and triple bonds [1]. The huge effort put in last decades to achieve their artificial synthesis, resulted in the development of different chemical and physical methods. The latter, in particular, show a higher scalability and ease of use, and so result to be more favourable within an industrial perspective. Among them, Pulsed Laser Ablation in Liquid (PLAL) is one of the most used and studied to synthesized polyynes [2]. This technique exploits the irradiation of a graphite target, immersed into a solvent, by a fs- or ns-laser. The large amount of energy delivered to the target generates a carbon plasma which, upon quenching by the liquid, results into the formation of sp-carbon chains [2].

The outstanding mechanical and transport properties of polyynes, that can be tuned by changing their length and terminations, make these systems highly appealing in view of future technological applications. Polyynes, un-

fortunately, easily undergo degradation phenomena like crosslinking reactions, which determines their sp-to-sp<sup>2</sup> transition, and oxidation [1]. Embedding polyynes inside solid polymeric matrices appears as a highly efficient strategy to stabilize them over long periods at ambient conditions [3, 4]. Moreover, the presence of metal nanoparticles aggregates inside these nanocomposite films has a twofold role, allowing to perform Surface Enhanced Raman Spectroscopy (SERS), fundamental to detect and characterize the embedded polyynes, as well as improve their stability [5]. However, still little is known about polyynes stability upon thermal treatments, and the goal of this work is to better understand this aspect. In particular, this work aims at the investigation, by SERS, of the thermal stability of polyynes, synthesized by PLAL and selected by length and terminations via High Performance Liquid Chromatography (HPLC), embedded in polyvinyl alcohol (PVA) polymeric nanocomposite films. Indeed, in sight of future technological applications, it is of fundamental importance to understand the thermal behaviour of these systems and how it is affected by their length and termi-

nations. In the preliminary part of this work, I optimized the Ag/PVA/polyynes nanocomposites composition and the SERS measurements parameters that allowed to perform SERS acquisitions with the highest signal-to-noise ratio without the risk of damaging the films. Then, I developed a methodology to perform the thermal treatment of the nanocomposite films and monitor polyynes thermal stability by means of a Peltier thermoelectric modulus coupled with an *in situ* SERS mapping procedure. From these results, I evaluated the roles of the length, the terminations and the chain-nanoparticle interaction on polyynes thermal stability.

## 2. Materials and Methods

Polyynes synthesis was performed through pulsed laser ablation in liquid. The setup is equipped with a Quantel Q-switched ns-pulsed Nd:YAG laser with a repetition rate of 10 Hz and a pulse duration of 6 ns. The ablations were performed by irradiating a graphite target immersed, respectively, in isopropyl-alcohol or dichloromethane with the aim to produce, respectively, H-capped and Cl-capped polyynes. All ablations were carried out at the fundamental harmonics of the laser, i.e. 1064 nm, with an energy per pulse set to 50 mJ, a fluence of  $2.71 \frac{J}{cm^2}$  and a duration of 30 minutes. The polyynes mixture obtained after each ablation was purified using cyclohexane through a chromatography column filled with Silica Gel 60 (0.063-0.200 mm), followed by phase transfer in acetonitrile, to make the mixture compatible with the HPLC aqueous mobile phase. Finally, the purified solution was concentrated through the use of rotavapor. A Shimadzu Prominence UFLC was employed to perform Reverse-Phase High Performance Liquid Chromatography (RP-HPLC), allowing to both detect and separate size-selected polyynes from the purified mixture. The injection volume was set to 30  $\mu$ L, and the employed chromatographic column was the Phenomenex Luna C18 (150 mm  $\times$  4.6 mm, 3  $\mu$ m particle size). The method selected for all the RP-HPLC runs was characterized by a duration of 45 minutes, and exploited a mobile phase gradient. The starting composition of the mobile phase was 35% water and 65% acetonitrile, while the final one was 5% water and 95% acetonitrile. A preliminary run allowed to identify

the elution times for all the polyynes of interest, helping their subsequent precise collection in different vials. PVA was selected as polymeric matrix due to its water solubility, high filmability and non-toxicity. Ag nanoparticles were obtained by means of the Lee-Meisel method, here implemented with the direct dissolution of PVA granules during nanoparticles formation. Ag/PVA/polyynes nanocomposites were obtained by mixing the size- and termination-selected polyynes with the Ag/PVA colloid, and their corresponding films were obtained by drop casting the nanocomposite solution itself on aluminium substrates. A Renishaw inVia Raman microscope with a diode-pumped solid-state laser (532 nm) was adopted to perform nanocomposite films characterization and *in-situ* SERS mapping. In particular, all spectral acquisitions were performed in static mode, employing a 20x or 50x microscope objective.

## 3. Experimental results

### 3.1. Films composition and SERS parameters

A preliminary study was performed to optimize both the Ag/PVA/polyne film composition and the SERS measurement parameters. It was proved the efficiency of the PLAL-produced mixtures purification process in polyynes stabilization. Indeed, both the mixtures obtained by performing the PLAL process into isopropyl-alcohol and dichloromethane showed an almost unchanged UV-Vis absorption spectrum after, respectively, 78 days and 50 days from the purification (Fig. 1). This great stabilization effect is justified by considering the removal of impurities and by-products performed through the solution purification, that prevents them from reacting with the polyynes, thus reducing the probabilities of crosslinking and degradation.

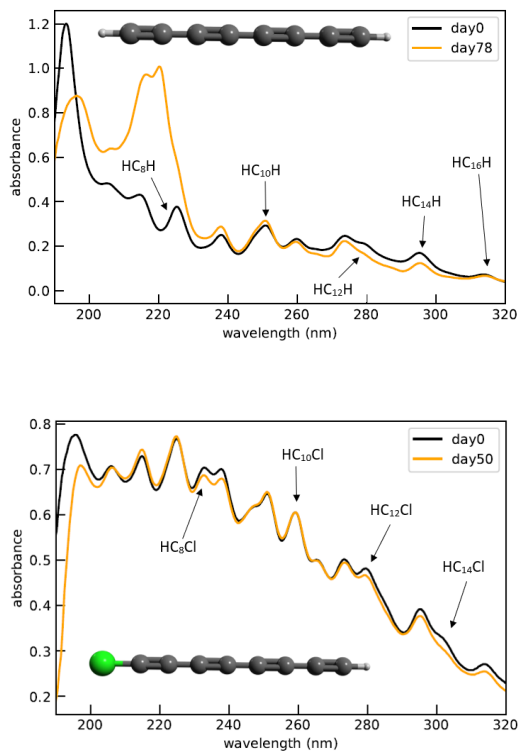


Figure 1: UV-Vis absorption spectrum of the purified H-capped (above) and Cl-capped (below) polyynes mixture. In black, the as purified mixture. In orange, the purified mixture after, respectively, 78 days and 50 days for the H- and Cl-capped polyynes mixtures. A simplified sketch of  $HC_8H$  and  $HC_8Cl$  chains is reported.

The composition of the Ag/PVA solution, obtained by dissolving the polymer during nanoparticles formation through the Lee-Meisel method, was optimized by adding 4% of the total solution weight of PVA. This quantity grants a good trade-off between solution viscosity, magnetic stirring ease, filmability, and PVA detection via SERS spectroscopy. Also the SERS measurement parameters have been optimized, finding a compromise between the laser power delivered to the nanocomposite sample and the duration of the spectral acquisitions that allowed to perform SERS analysis with the highest signal-to-noise ratio in a reasonable amount of time without the risk of burning the films. Specifically, the optimized spectral acquisitions were performed in static mode with the 532 nm Raman laser, a 50x microscope objective, and a grating of 1800 lines/mm, covering a frequency range from 1750 to 3180  $cm^{-1}$ . This spectral windows allows to monitor both the SERS band

of polyynes and the CH stretching peak of PVA. The comparison of the SERS spectra of the nanocomposites obtained by mixing polyynes and Ag/PVA solutions in a volume ratio of 1:2 and 1:10, performed with the optimized parameters described above, allowed me to establish a correlation between the relative amount of polyynes and nanoparticles that maximised polyynes SERS signal and stability. A "homogenisation" of the polyynic SERS signals is observed passing from 1:10 to 1:2 volume ratio (Fig. 2), with the obtainment equalized SERS signals independently from the specific polyyne originally embedded into the nanocomposite. This was interpreted as the consequence of the more favoured chain-chain crosslinking occurring in presence of higher polyynes concentration. Due to this degradative phenomenon,  $sp^2$  complexes would be generated, and their interaction with the Ag nanoparticles aggregates would provide equalized SERS signals, independently from the specific polyyne embedded into the nanocomposite. To improve the stability of polyynes in nanocomposites and, as a consequence, restore the signal distinguishability, a films composition optimization method was developed. In this sense, by setting a constant molar ratio ( $R$ ) between polyynes and nanoparticles, i.e.  $R = 7.13 \cdot 10^{-4}$ , I could achieve polyynes stability (distinguishability) and the maximisation of their SERS bands intensity (Fig. 3). The different behaviour observed when dealing with the most concentrated  $HC_nH$  and  $HC_nCl$  polyynes is justified by a different interaction strength between the chlorine and the hydrogen terminations with the Ag nanoparticles, based on electronegativity considerations. Indeed, considering the Ag nanoparticles as a source of electrons, I assumed a stronger interaction between them and chlorine, due to its much higher electronegativity compared to that of hydrogen. As a consequence, a smaller amount of Ag nanoparticles is required in the case of  $HC_nCl$ -based nanocomposites (e.g. 45  $\mu L$  for  $HC_8Cl$ ) compared to  $HC_nH$  ones (e.g. 300  $\mu L$  for  $HC_8H$ ) to obtain the same results.

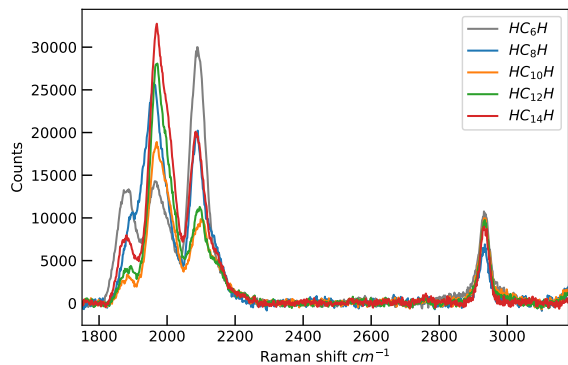


Figure 2: SERS spectra of 1:2 films embedding size-selected H-capped polyynes with the optimized SERS parameters.

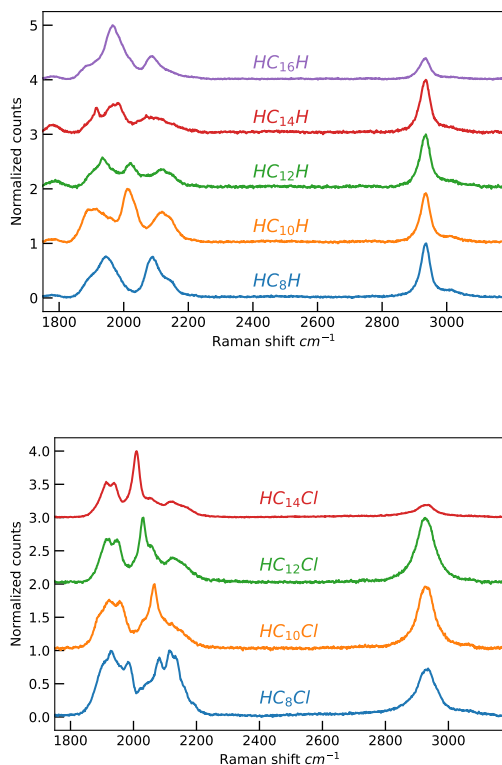


Figure 3: Normalized SERS spectra of nanocomposite films embedding H-capped (above) and Cl-capped (below) polyynes of different lengths with optimized composition.

### 3.2. Thermal stability of polyynes monitored via *in situ* SERS mapping

I designed and developed a new methodology to perform the thermal treatment of the nanocomposite films and to monitor simultaneously the thermal stability of the embedded polyynes, by

means of a Peltier thermoelectric modulus coupled with an *in situ* SERS mapping process. Being the synthesized films inhomogeneous, this methodology, involving the use of SERS mapping to monitor their response to the thermal treatment, allowed to obtain their reliable statistical description, permitting also to perform long SERS measurements without damaging them. The Peltier thermoelectric modulus, placed onto a heat dissipation system, heated up the film under analysis, and a thermocouple tracked its temperature during the whole thermal treatment, i.e., for 45 minutes, corresponding also to the SERS mapping time. Moreover, I established a procedure to determine the effect of the Raman laser on the stability of H-capped polyynes inside their nanocomposite films, allowing to decouple the thermal and laser-induced effects on their degradation.

First, the thermal stability of the PVA polymeric matrix was assessed, demonstrating its capability to sustain the thermal treatment up to 100°C, much above its glass transition temperature (85°C). All the nanocomposite films, instead, were subjected to two SERS maps, a preliminary map at room temperature and, just after, an *in situ* map during the sample heating. The thermal treatments were carried out at 60°C, 80°C, and 100°C for all nanocomposites. After a rapid transient, the temperature reached by the Peltier modulus was maintained constant during the whole thermal treatment. The integrated area corresponding to the frequency range of the SERS band of the embedded polyne, i.e. 1850-2220  $\text{cm}^{-1}$ , was evaluated for each spectrum. Setting as  $a_0$  and  $a_1$ , respectively, the polyynic integrated area computed before and during the thermal treatment, the ratio  $a_1/a_0$  was plotted as a function of the mapping time for each nanocomposite. I recorded six spectra on each of four points of each H-polyne based film with the same SERS parameters of the maps, to determine the laser heating effect on H-capped polyynes' thermal stability. One minute interval was set between each acquisition, to experimentally simulate the film recovery from the laser heating between the two SERS maps. To correct the laser effect only for the *in situ* SERS map, being the one embodying both the thermal and the laser effects, the area of the  $n = 2$  acquisition was equalized to that of

the  $n = 1$  acquisition through a "correction factor"  $f$  extracted from the exponential decay fit applied to the described plots. Once performed the fit of each point dataset (i.e. six acquisitions per point), the adimensional "correction factor"  $f$  was extracted for each polyne, by averaging those calculated from the other points (i.e. four per nanocomposite film). To separate the degradation due to the laser from the thermal one, the integrated area evaluated during the thermal treatment ( $a_1$ ) of the embedded polyne was multiplied by the corresponding mean correction factor. As expected, being the value of the mean decoupling factor always  $> 1$ , the resulting  $a_1/a_0$  ratio was increased with respect to the original one (e.g.  $HC_{10}H$  in Fig. 4).

The thermal stability of the different polyynes embedded in the nanocomposite films was, thus, evaluated by looking at the evolution of the  $a_1/a_0$  SERS ratio during the thermal treatments at different temperatures. This analysis was performed with laser-corrected ratios for hydrogen-capped polyynes, while for chlorine-capped polyynes, for which no laser heating effect was available, pristine data (without laser correction) were used. Independently from their terminations, the investigated chains showed a similar  $a_1/a_0$  ratio trend as a function of the thermal treatment temperature. In particular, a slow ratio reduction was observed at  $60^\circ\text{C}$ , followed by a faster degradation at  $80^\circ\text{C}$  and by an evident exponential decay trend at  $100^\circ\text{C}$  (e.g.  $HC_{10}H$  in Fig. 5), already visible at  $80^\circ\text{C}$  only for  $HC_{16}H$ . The thermal degradation process affecting the polyynes embedded in the nanocomposite films, when subjected to high temperatures, is thought to occur in two phases. During the first, the  $a_1/a_0$  ratio decreases rapidly due to the fast polyynes degradation resulting from the high increase in temperature. Then, its reduction becomes very slow, approaching an almost constant value during the whole remaining thermal treatment time. This slowdown in polyynes degradation was justified by assuming chains stabilizing effect determined by the eventual formation of more stable sp-sp<sup>2</sup> complexes, already described above. Considering the different chain terminations, it was possible to observe a much higher thermal resistance of the Cl-capped polyynes with respect to the hydrogenated ones. Indeed,

contrarily to  $HC_nH$ -based films, where an already marked degradation was visible at  $80^\circ\text{C}$ ,  $HC_nCl$ -based films showed, independently from their length, very high stability up to  $80^\circ\text{C}$ , almost unchanged with respect to the one found at  $60^\circ\text{C}$  (e.g.  $HC_{10}Cl$  in Fig. 6). The higher stability of Cl-capped polyynes can be justified by a stronger interaction between Ag nanoparticles and chlorine, the smaller amount of nanoparticles present in  $HC_nCl$  based nanocomposites, and so their smaller localized heating effect, and the larger steric hindrance of chlorine terminations, which help stabilizing the sp-chains.

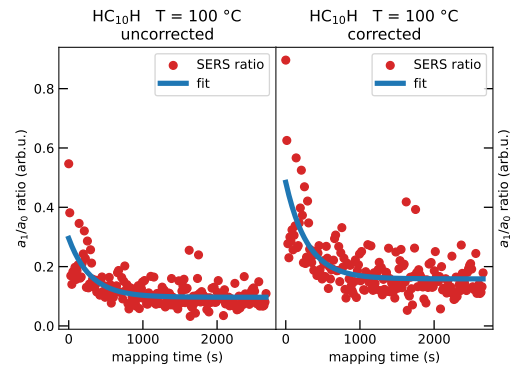


Figure 4:  $HC_{10}H$   $a_1/a_0$  ratio plotted as a function of the mapping time without (left) and with (right) laser correction.

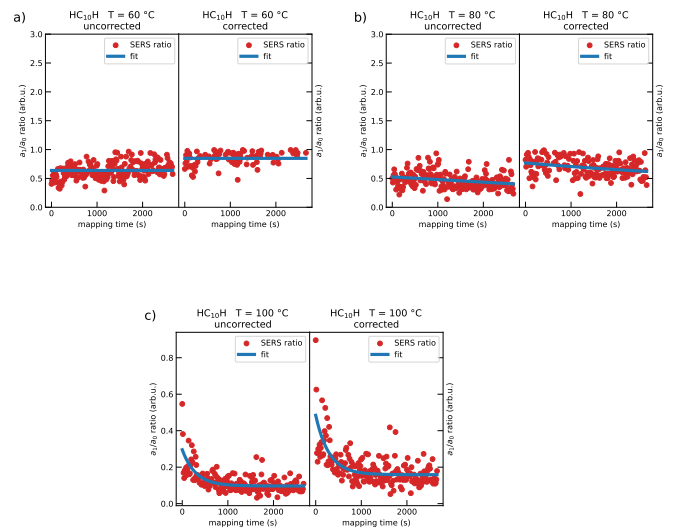


Figure 5:  $HC_{10}H$   $a_1/a_0$  ratio as function of the mapping time, performed at  $60^\circ\text{C}$  (a),  $80^\circ\text{C}$  (b),  $100^\circ\text{C}$  (c). The uncorrected ratio is on the left and the laser-corrected is on the right.



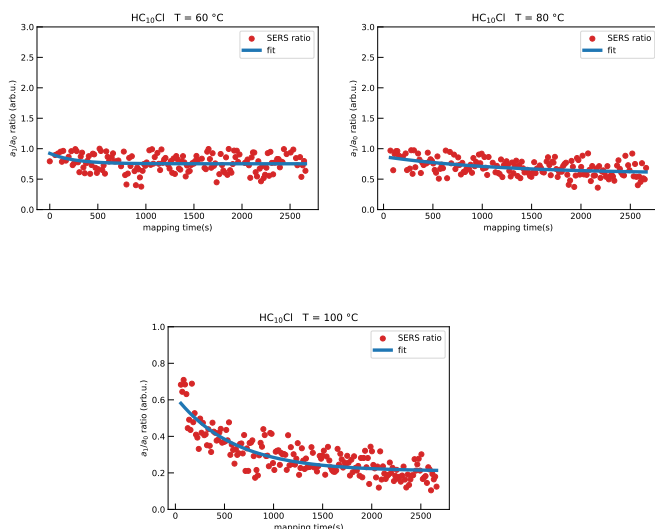


Figure 6:  $HC_{10}Cl$   $a_1/a_0$  ratio plotted as function of the mapping time. Plots obtained by performing the *in situ* SERS map at 60°C (a), 80°C (b), 100°C (c) are shown.

#### 4. Conclusions

In this work, a strategy to optimize the nanocomposite films composition was developed, and proved to be effective independently from the concentration of the embedded HPLC-collected polyynes. In particular, a relationship between the relative amount of polyynes and Ag nanoparticles and the polyynes stabilization within the nanocomposites was demonstrated. A new methodology was also developed to assess the thermal stability of the size- and termination-selected polyynes embedded in PVA nanocomposite films by a Peltier thermoelectric modulus coupled with an *in situ* SERS mapping procedure. The main advantages of this methodology were the possibility to perform long SERS measurements on the films without damaging them, and eliminate the issue resulting from films inhomogeneity, allowing for a statistical description of the samples SERS signal and thermal stability. Longer chains and higher thermal treatments temperatures resulted in faster polyynes degradation processes in both H-capped and Cl-capped polyynes based films. Cl-capped polyynes demonstrated a much larger thermal stability compared to H-capped ones, and this can be justified by a stronger interaction between Ag nanoparticles and chlo-

rine atoms, the smaller localized heating effect provided to the embedded polyynes due to the smaller amount of Ag nanoparticles present in  $HC_nCl$  based nanocomposites, and the larger steric hindrance of the chlorine terminations with respect to hydrogen ones, which can reduce the probability of crosslinking. The laser heating effect on H-polyynes stability was also investigated and seemed to play a non negligible role in their degradation. However, it was possible to decouple the thermal and laser effects on H-polyynes based nanocomposites providing a clearer understanding of the effect of the thermal treatment alone on their stability.

#### References

- [1] Casari et al. Carbon-atom wires: 1-d systems with tunable properties. *Nanoscale*, 8(8):4414–4435, 2016.
- [2] Marabotti et al. Pulsed laser ablation in liquid of sp-carbon chains: status and recent advances. *Chinese Physics B*, 2022.
- [3] Peggiani et al. In situ synthesis of polyynes in a polymer matrix via pulsed laser ablation in a liquid. *Materials Advances*, 1(8):2729–2736, 2020.
- [4] An et al. Stability improvement of c8h2 and c10h2 embedded in poly (vinyl alcohol) films with adsorption on gold nanoparticles. *Chemical Physics Letters*, 637:71–76, 2015.
- [5] Casari et al. Stabilization of linear carbon structures in a solid ag nanoparticle assembly. *Applied physics letters*, 90(1):013111, 2007.